

# IceCube Neutrinos from Hadronically Powered Gamma-Ray Galaxies

Andrea Palladino, Anatoli Fedynitch, Rasmus W. Rasmussen, Andrew M. Taylor  
*DESY, Platanenallee 6, 15738 Zeuthen, Germany*

(Dated: December 13, 2018)

In this work we use a multi-messenger approach to determine if the high energy diffuse neutrino flux observed by the IceCube Observatory can originate from  $\gamma$ -ray sources powered by Cosmic Rays interactions with gas. Typical representatives of such sources are Starburst and Ultra-Luminous Infrared Galaxies. Using the three most recent calculations of the non-blazar contribution to the extragalactic  $\gamma$ -ray background measured by the Fermi-LAT collaboration, we find that a hard power-law spectrum with spectral index  $\alpha \leq 2.12$  is compatible with all the estimations for the allowed contribution from non-blazar sources, within  $1\sigma$ . Using such a spectrum we are able to interpret the IceCube results, showing that various classes of hadronically powered  $\gamma$ -ray galaxies can provide the dominant contribution to the astrophysical signal. With the addition of neutrinos from the Galactic plane, it is possible to saturate the IceCube signal. Our result reverses previous findings in which evidence was claimed against hadronic sources being the dominant source of IceCube neutrinos.

*Introduction.*— The IceCube Collaboration has detected a diffuse high-energy astrophysical neutrino flux [1]. However, despite the six years since its detection, its origin remains unclear. Several candidate source populations have been proposed, such as blazars [2–4],  $\gamma$ -Ray Bursts (GRBs) [5–8], Star Forming Galaxies and Starburst Galaxies [9–12], dark matter decay [13, 14] or Galactic sources, like Galactic center [15–17], Galactic plane [18–20], Galactic halo [21]. Some models are strongly constrained by the absence of correlations between the directions of the high-energy neutrinos and known sources. This result is compatible with neutrino-bright sources being dim photon sources. For example, distant blazars that are not resolved by the Fermi satellite due to their low luminosity, could have a high fraction of interacting protons and thus be efficient neutrino sources [22]. GRBs with choked jets are another type of  $\gamma$ -ray dim and neutrino-bright sources [23]. So far, only one neutrino source candidate has been tentatively identified, the blazar TXS 0506+056 [24], one of the brightest blazars located at a redshift  $z = 0.34$ .

The multi-messenger approach can be applied in various ways, either on a “per source” basis where a single object is studied simultaneously in multiple wavelengths, in neutrinos and in gravitational waves. Alternatively, one can also study the entire populations of sources using diffuse (time and angular integrated) fluxes of neutrinos and photons, where the relative differences between observed energy spectra can constrain certain scenarios. The latter approach has been recently applied to study the contribution of Star Forming Galaxies (SFG), including Starburst and Star-Forming Active Galactic Nuclei, to the diffuse neutrino flux [12]. The study concluded that these sources can only contribute at most a few percent of the observed neutrinos, essentially excluding SFGs as the dominant sources of high-energy neutrinos in IceCube. Since the  $\gamma$ -ray radiation in SFGs predominantly originates from Cosmic Ray interactions with gas,

the result may be generalized to the extent that proton-proton ( $pp$ ) interactions can not be the main mechanism of astrophysical neutrino production.

In astrophysical environments where  $pp$  interactions dominate cosmic ray cooling, the relation between the  $\gamma$ -ray and the neutrino emission is fixed. With approximately equal numbers of  $\pi^+$ ,  $\pi^-$  and  $\pi^0$  being produced in high-energy collisions, the total energy budget of  $\gamma$ -rays is 2/3 of the total energy budget of neutrinos. If these “hadronic sources” power the entire diffuse neutrino flux, it is sufficient that only a subset of all galaxies significantly contributes, in line with the requirement for a high-energy cutoff of  $E_\nu \sim \text{few PeV}$ . Such sources are likely to carry characteristics of Starburst galaxies (SBG) such as enhanced stellar light and dust production, which results in infrared luminosities 10-100 times higher compared the more abundant normal galaxies [25]. In reality, this heightened level of infrared galaxies is a continuum, with even higher values observed in what are classified as Ultra-Luminous Infrared Galaxies (ULIRGs), which are more luminous (infrared luminosity 100-1000 higher than normal Galaxies, see Fig.1 of [26]) but less numerous. Fermi reveals an almost linear correlation between the infrared and the  $\gamma$ -ray luminosities [26, 27]. Therefore, “infrared bright” galaxies like Starburst and ULIRGs are good candidates of Hadronically powered  $\gamma$ -ray Galaxies (HAGS). The neutrino and  $\gamma$ -ray spectrum from these objects is expected to be a power law, whose spectral index remains uncertain in the relevant energy range (above 50 GeV), since only a few members of the broad HAGS source class (NGC253, M82) have been detected up to very high energies. We will therefore consider the spectral index as a free parameter in the present work, keeping in mind that the observation of NGC253 suggests an  $\sim E^{-2.15 \pm 0.10}$  above 50 GeV, which is the energy region relevant for our purpose (see Fig. 2).

This work aims to re-evaluate the compatibility of the

most recent neutrino observations by IceCube with an origin from HAGS. We apply a multi-messenger method and combine the diffuse extragalactic  $\gamma$ -ray background (EGB) observations by Fermi with the throughgoing muon energy flux measured by IceCube. Then we also evaluate the agreement with other two IceCube dataset, where low energy events (down to  $\sim$  TeV) are contained.

*Methods.*— We start with a comparison of the three IceCube data analyses, namely: *i) the through-going muons (TGM) [28, 29]* originating from muon neutrino and anti-neutrino interactions outside the detector. This selection contains tracks from the opposite (Northern) hemisphere and at a higher energy threshold of 200 TeV; *ii) the high-energy starting events (HESE) [30, 31]*, characterized by an interaction vertex contained in the fiducial detector volume. HESE contain shower and track like events mostly coming from the Southern hemisphere; *iii) the 4-year cascade (CAS<sub>4</sub>) [32]* sample contains neutrinos of all flavors interacting with a cascade topology, *i.e.* mostly electron and tau neutrinos. The energy threshold is the lowest for this dataset, around  $\sim$  TeV energies.

We notice that above 200 TeV both throughgoing muons and HESE suggest a hard power law spectrum  $d\Phi_\nu/dE \propto E^{-2.2 \pm 0.1}$ . Since above this energy the contribution coming from the atmospheric background is small ( $\sim$  20% using the signalness reported in Tab.4 of [28]), we assume that this flux is representative of the true astrophysical signal. On the other hand one cannot neglect the information coming from the spectrum measured below 200 TeV; therefore, at the end of our multi-messenger analysis, we subsequently evaluate the compatibility between our findings with low energetic HESE and CAS<sub>4</sub> datasets.

In order to compute the diffuse neutrino and  $\gamma$ -ray fluxes we make use of the relation, in which the energy budget in neutrinos is 3/2 of that in  $\gamma$ -rays. We assume for the density of the hadronic sources an evolution  $\rho(z) = \rho_0(1+z)^m$ , with  $m = 3.4$  for  $z < 1$  and  $m = -0.5$  up to  $z = 4$ , like the star forming rate [33]. The diffuse all-flavor neutrino flux  $\phi_\nu$  is, therefore, related to the product of the local source density  $\rho$  and the luminosity at 100 GeV  $\mathcal{L}_{100 \text{ GeV}}$ , *i.e.* to the local emissivity:

$$\begin{aligned} \frac{d\Phi_\nu(E)}{dE} &= \int dz \frac{\rho(z)}{H(z)} \frac{d\phi_\nu}{dE}(E(1+z)) \\ &= \int dz \frac{\rho(z)}{H(z)} \frac{3}{2} \frac{d\phi_\gamma}{dE}(E(1+z)) \\ &\approx \Phi_0 \left( \frac{\rho_0}{\rho_0(\alpha)} \right) \left( \frac{\mathcal{L}_{100 \text{ GeV}}}{\mathcal{L}_{100 \text{ GeV}}^{\text{NGC253}}} \right) \left( \frac{E}{100 \text{ TeV}} \right)^{-\alpha^*} e^{-E/E_{\text{cut}}^*(\alpha)}, \end{aligned} \quad (1)$$

where  $\Phi_0$  is constant and equal to  $3 \times 10^{-18} \text{ GeV}^{-1} \text{ cm}^{-2} \text{ s}^{-1} \text{ sr}^{-1}$ ,  $\mathcal{L}_{100 \text{ GeV}}^{\text{NGC253}} = (5 \pm 2) \times 10^{39} \text{ erg/s}$  is the  $\gamma$ -ray luminosity of NGC253 at 100 GeV [34], which we use here as a HAGS prototype.

We determine the spectral-index dependent local ( $z = 0$ ) source density  $\rho_0(\alpha)$  by fitting the astrophysical neutrino signal to the TGM spectrum in the range 0.1 – 1 PeV. More details on the calculation are reported in the supplementary material. We assume throughout that the spectrum of neutrinos and  $\gamma$ -rays at the sources is described by a power-law with a spectral index  $\alpha$  and an exponential cutoff energy  $E_{\text{cut}}$ . The spectral index remains approximately the same at Earth while the energy cutoff is slightly different and we denote it with  $E_{\text{cut}}^*$ . The values of  $\rho(\alpha)$  and  $E_{\text{cut}}^*(\alpha)$ , given in Tab.II, are discussed in the result section.

In the computation of the diffuse  $\gamma$ -ray flux the interactions with the Extragalactic Background Light (EBL) have to be taken into account. The high-energy photons are absorbed and reprocessed through electromagnetic cascades, resulting in the re-appearance of this energy flux at lower energies. We use the same source spectrum as for the neutrinos, offset by 2/3 coming from energy budget considerations (see Eq. (2)). The transport of gamma rays through the intergalactic medium yields two components at the observer  $\phi_\gamma = \phi_\gamma^{\text{dir}} + \phi_\gamma^{\text{casc}}$ . The direct component here arrives from the source population, and is attenuated at high energies by the EBL. This attenuation feeds electromagnetic cascades, giving rise to the cascade component at energies below a few hundred GeV. We use [35] for the EBL model and the method given in [36] to compute the electromagnetic cascade during the propagation.

The resulting propagated  $\gamma$ -ray flux has to be compared with the non blazar component of the extragalactic gamma-ray background (EGB). This residual component of the EGB was estimated by the Fermi collaboration [37]. The remaining (non-blazar) fraction, is thought to be shared by all the other  $\gamma$ -ray emitters, such as normal and starburst galaxies and misaligned blazars. The share between the blazars and the non-blazar contribution varies between the different analyses, and are accompanied by large errors: the Fermi collaboration identifies the contribution from blazars to the EGB above 50 GeV as  $86\%_{-14}^{+16}$ % [37]; Lisanti et al. [38] as  $68\%_{-8}^{+9}$ % and Zechlin et al. [39] as  $81\%_{-19}^{+52}$ %. The cumulative  $\gamma$ -ray flux at Earth  $\phi_\gamma(\alpha)$  non-trivially depends on the spectral index of the source prototype since the share between the direct  $\phi_{\text{dir}}(\alpha)$  and the cascade  $\phi_{\text{casc}}(\alpha)$  components change. We evaluate the compatibility of HAGS with the non-blazar contribution by comparing the  $\gamma$ -ray flux integrated above 50 GeV with the integral of the EGB flux in the same energy range.

*Results.*— We check the compatibility of our model with the TGM energy flux by scanning over the source spectral index  $\alpha$  and by performing fits of the local density  $\rho_0(\alpha)$  of HAGS that maximize the throughgoing muon energy flux. We remark that throughgoing muons represent the cleanest way to observe astrophysical neu-

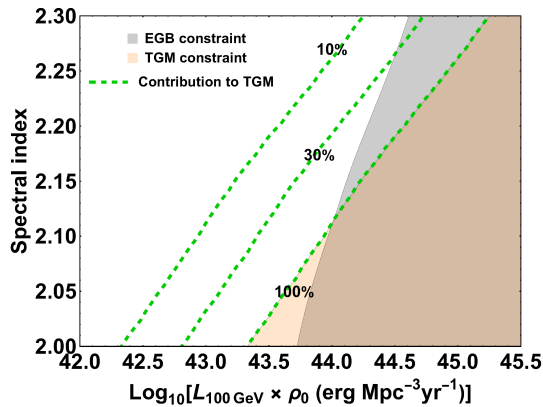


FIG. 1. Summary of our main results. The grey band represents the region excluded taking into account the non blazar contribution to the EGB calculated by Fermi [37]. The orange band represents the region excluded by integrating the throughgoing muon flux multiplied by energy between 200 TeV and 5 PeV, requiring that the energy budget predicted by our model is below the one measured by throughgoing muons. The green lines denote different contributions to the TGM energy flux.

trinos, since atmospheric muons are not present and the 200 TeV energy threshold reduces the contribution of atmospheric neutrinos. Moreover no contamination from the Galactic plane is expected.

In Fig.1 we report our result for different spectral indices and different luminosity densities. The bands represent forbidden regions at  $1\sigma$ . The gray region indicates the exclusion of the model by its contribution to the most pessimistic non-blazar estimation of the EGB. The orange band limits the allowed neutrino energy flux integrated between 200 TeV and 5 PeV with respect to what is maximally allowed by the TGM measurements. The dashed green lines represent partial contributions to the TGM energy flux. The result is valid for generalized  $pp$  sources, since the luminosity density is given by the product between the source density at redshift  $z = 0$  and the luminosity of the sources at 100 GeV. More details are reported in Tab.II of the supplementary material. For harder spectrum and the two HAGS prototypes, the starburst galaxy NGC253 and the ULRIG Arp220 (with a luminosity 100-150 times higher than NGC [26]), we find the local densities (given in Tab.II) to be compatible with the expectation for such sources.

As demonstrated in the Supplementary Material, normal galaxies contribute very little to the diffuse  $\gamma$ -ray and the neutrino fluxes due to their soft spectral indices and low luminosities. Our result places an upper limit on the source spectral index, with values of  $\alpha > 2.3$  being excluded at  $5\sigma$ , thus confirming the findings by [12] who based their arguments on the soft single power-law fit to the HESE data available at that time. On the contrary, we find that a source spectral index  $\alpha \leq 2.12$  is

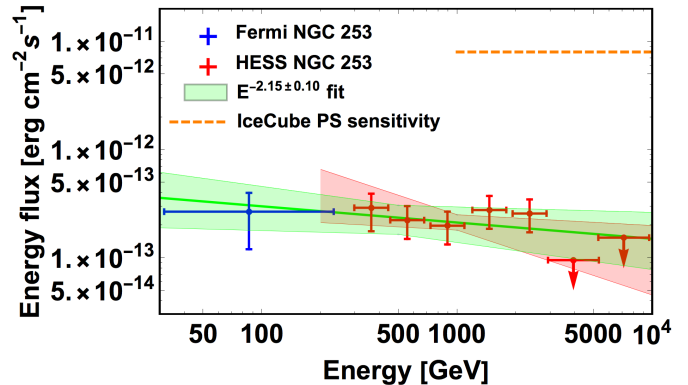


FIG. 2. The spectrum of the starburst galaxy NGC 253 from a combined analysis of Fermi (blue points) and HESS (red points and red band) [34]. The green band represent the flux above 50 GeV. The observed data points are well fitted by an  $E^{-2.15 \pm 0.10}$  spectrum, with an uncertainty of  $\sim 25\%$  on the normalization. The IceCube 7-year point source limit for a harder  $E^{-2}$  spectrum and NGC253's declination  $\delta \simeq -25^\circ$  is represented by the dashed line [41].

found to be compatible with the three estimations of the non blazar contribution within  $1\sigma$ . Moreover an index of  $\alpha = 2.12$  allows the saturation of the throughgoing muon energy flux.

We note here that this discussion on the contribution to the non-blazar of the EGB neglects the inevitable contribution from misaligned AGN. An estimation of the level of this component is in the range between 4% and 40% [40], with a best fit value of 12%. Taking this into account the remaining non AGN contribution would sit at level of 16%. Even for such a reduced level we still find compatibility with the throughgoing muon energy flux using a hard spectrum ( $\alpha = 2$ ) (see Appendix, Tab.II).

On the other hand a too hard spectrum is disfavored by the observation of the Starburst Galaxy NGC 253. The update measurements, provided by Fermi and HESS [34], suggest an  $E^{-2.15 \pm 0.10}$  spectrum above 50 GeV, i.e. our energy region of interest (see Fig.2). Therefore as a baseline spectrum we choose  $\alpha = 2.12$ , *i*) being the softest spectrum that is able to saturate the TGM energy flux, *ii*) without producing any tension with the non blazar contribution, *iii*) being compatible with the recent update on the observation result of NGC 253.

Figure 3 confirms that a neutrino spectrum of the form  $dN/dE_\nu \propto E_\nu^{-2.12}$  with a source energy cutoff at 10 PeV is well in agreement with the TGM measurement and with the high-energy part of HESE. Smaller cutoff values are generally found to yield a better compatibility with the EGB, gradually falling short in explaining the highest energy neutrinos. An energy cutoff of 10 PeV for neutrinos at the source corresponds to an average cutoff of 200 PeV for protons. According to [9], SBGs may be capable of accelerating protons to such high energies, supporting the compatibility of HAGS with the multi-

messenger observations. Alternatively, a more effective accelerator members of the HAGS class is discussed in [42]. Contrary to these expectations, recent indications by the two Ultra-High Energy Cosmic Ray (UHECR) observatories see first indications for a directional correlation between the arrival directions of cosmic rays above 39 EeV and nearby SBG [43, 44]. Should HAGS be the sources of these UHECR, the local abundance of sources capable of reaching 200 PeV should be rather high.

*Comparison with low energy events:* We check the compatibility of our result with the other IceCube dataset. Concerning the low energy measurements, the expected number of HESE events are reported in Table I. Using the HESE effective areas [1] and our baseline spectrum, we find that HAGS can account for 33 out of about 41 astrophysical signal events, obtained by subtracting the  $\sim 41$  expected background events from the 82 detected events in HESE [29]. While the event counts are well described by our model, the hard spectrum undershoots the second HESE bin, leaving space for other small contributions from other sources or background in this energy range. A possible additional contribution may come from the Milky Way’s galactic disc can be present among the events below 100 TeV from the Southern hemisphere. Galactic neutrinos are expected to give a contribution below  $\sim 150$  TeV, reflecting the possible  $\sim 3$  PeV knee of the primary proton spectrum [18, 20, 45]. The current estimates predict  $\sim 1$  neutrino/year in the HESE dataset (above 30 TeV), in line with the latest experimental limits [46]. Together with the galactic component, our model saturates the HESE signal event count to 94% at the best fit.

We also compare our result with the differential event distribution of the CAS<sub>4</sub> sample. This comparison requires a more technical discussion, that is reported in the Appendix. Using the baseline spectrum we find this model to be compatible within the uncertainties.

*Conclusion.* — We applied a multi-messenger approach to study the contribution of HAGS to IceCube’s diffuse neutrino flux combining the constraints from current  $\gamma$ -ray and neutrino observations. HAGS are (typically) infrared bright sources with a hard  $\gamma$ -ray spectrum from proton-proton interactions, for which the relation to the expected neutrino flux is well defined. The strongest constraint comes from the non-blazar contribution to the extragalactic  $\gamma$ -ray background.

We find that a hard power-law spectrum with an index  $\alpha \leq 2.12$  and an energy cutoff at 10 PeV at the source to be compatible with the currently available estimations of the non-blazar contribution. In particular, due to the large uncertainties of these estimates it is impossible to derive tighter constraints solely from  $\gamma$ -ray observations and exclude HAGS, which include Starburst Galaxies and ULIRGs, as the dominant sources of diffuse neutrinos. Moreover, this conclusion remains valid even when an estimation of the misaligned AGN are further removed

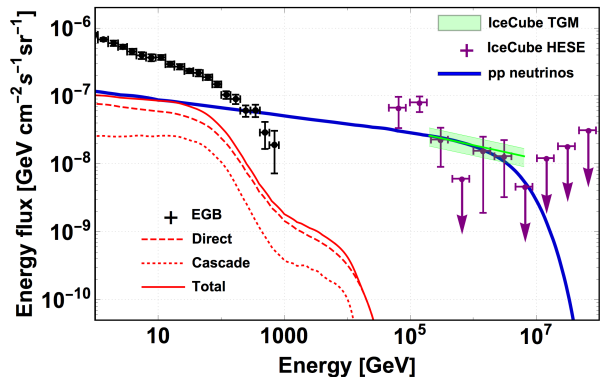


FIG. 3. Diffuse extragalactic neutrino and  $\gamma$ -ray fluxes from a population of HAGS, using our baseline spectrum ( $\alpha = 2.12$ ) and 10 PeV as the energy cutoff at the source. The latest HESE data is indicated by the purple points [31] and the TGM energy flux by the green band [47]. The black data points show the total Fermi EGB [48]. The  $\gamma$ -ray flux associated with HAGS is shown separately for the direct and the cascade fractions (red curves). The red curves are below the measurement since the integral flux above 50 GeV from HAGS can not exceed the non-blazar contribution accounting for a few tens of % of the entire EGB.

TABLE I. Decomposition of the 5.7 years of the 82 HESE events [31] into different source components. The background events are given by IceCube in [29], whereas the Galactic neutrinos are computed in [19] and they are roughly 1 per year in the HESE dataset. Neutrinos from HAGS accounts for 33 of the 41 signal events, i.e. about 80% of the astrophysical signal.

	Expected	Fraction
Atmospheric muons	$25.2 \pm 7.3$	$32\% \pm 9\%$
Atmospheric neutrinos	$15.6^{+11.4}_{-3.9}$	$20\%^{+14\%}_{-5\%}$
Extragal. neutrinos (HAGS)	$33 \pm 8$	$41\% \pm 10\%$
Galactic neutrinos	$\leq 5.7$	$\leq 7\%$
Total	$79.5^{+15.9}_{-11.7}$	—

from the extragalactic  $\gamma$ -ray background.

Such a spectrum is also found to be consistent with the spectrum of the NGC253 (a prototype of HAGS) above 50 GeV and with both the throughgoing muon energy flux detected by IceCube and the high energy part of the HESE flux. We also evaluated the contribution of our baseline spectrum to the low energy part of the HESE and CAS<sub>4</sub> events. We do not find any contradiction between the hypothesis that the dominant contribution of the IceCube neutrino energy flux comes from HAGS, since they can fully power the throughgoing muon energy flux and contribute to the majority of the signal neutrinos contained in HESE. The small remaining fraction can be attributed to neutrinos from the Milky Way’s galactic plane. Due to the soft spectral index and low maximal energies, the contribution from an entire population of “normal galaxies” (like ours) is at the few % level.

This result reverses the conclusions drawn in previous studies, which found evidence against “Star Forming Galaxies” [12] as the major source of IceCube neutrinos.

Compared to the brightest  $\gamma$ -ray sources (like blazars) HAGS are comparatively dim steady emitters, with their detection as neutrino sources requiring neutrino detectors with at least an order of magnitude more sensitivity compared to IceCube’s current sensitivity. In the  $\gamma$ -ray domain, the upcoming Cherenkov Telescope Array (CTA) will be able to discover more nearby HAGS, as well as extend the energy spectral energy range up to higher energies of those already detected. Being hadronic sources, HAGS are natural candidates for this neutrino emission. We find good compatibility of HAGS being the dominant neutrino source class.

**Acknowledgments.** This project has received funding from the European Research Council (ERC) under the European Union’s Horizon 2020 research and innovation programme (Grant No. 646623).

- 
- [1] M. G. Aartsen et al. (IceCube), *Science* **342**, 1242856 (2013), arXiv:1311.5238 [astro-ph.HE].
- [2] R. J. Protheroe, *ASP Conf. Ser.* **121**, 585 (1997), arXiv:astro-ph/9607165 [astro-ph].
- [3] W. Essey, O. E. Kalashev, A. Kusenko, and J. F. Beacom, *Phys. Rev. Lett.* **104**, 141102 (2010), arXiv:0912.3976 [astro-ph.HE].
- [4] K. Murase, Y. Inoue, and C. D. Dermer, *Phys. Rev. D* **90**, 023007 (2014), arXiv:1403.4089 [astro-ph.HE].
- [5] B. Paczynski and G. H. Xu, *Astrophys. J.* **427**, 708 (1994).
- [6] E. Waxman and J. N. Bahcall, *Phys. Rev. Lett.* **78**, 2292 (1997), arXiv:astro-ph/9701231 [astro-ph].
- [7] S. Huemmer, P. Baerwald, and W. Winter, *Phys. Rev. Lett.* **108**, 231101 (2012), arXiv:1112.1076 [astro-ph.HE].
- [8] K. Murase and K. Ioka, *Phys. Rev. Lett.* **111**, 121102 (2013), arXiv:1306.2274 [astro-ph.HE].
- [9] G. E. Romero and D. F. Torres, *Astrophys. J.* **586**, L33 (2003), arXiv:astro-ph/0302149 [astro-ph].
- [10] A. Loeb and E. Waxman, *JCAP* **0605**, 003 (2006), arXiv:astro-ph/0601695 [astro-ph].
- [11] I. Tamborra, S. Ando, and K. Murase, *JCAP* **1409**, 043 (2014), arXiv:1404.1189 [astro-ph.HE].
- [12] K. Bechtol, M. Ahlers, M. Di Mauro, M. Ajello, and J. Vandenbroucke, *Astrophys. J.* **836**, 47 (2017), arXiv:1511.00688 [astro-ph.HE].
- [13] A. Esmaili and P. D. Serpico, *JCAP* **1311**, 054 (2013), arXiv:1308.1105 [hep-ph].
- [14] M. Chianese, G. Miele, S. Morisi, and E. Vitagliano, *Phys. Lett. B* **757**, 251 (2016), arXiv:1601.02934 [hep-ph].
- [15] S. Razzaque, *Phys. Rev. D* **88**, 081302 (2013), arXiv:1309.2756 [astro-ph.HE].
- [16] M. Ahlers and K. Murase, *Phys. Rev. D* **90**, 023010 (2014), arXiv:1309.4077 [astro-ph.HE].
- [17] S. Celli, A. Palladino, and F. Vissani, *Eur. Phys. J. C* **77**, 66 (2017), arXiv:1604.08791 [astro-ph.HE].
- [18] A. Palladino and F. Vissani, *Astrophys. J.* **826**, 185 (2016), arXiv:1601.06678 [astro-ph.HE].
- [19] G. Pagliaroli, C. Evoli, and F. L. Villante, *JCAP* **1611**, 004 (2016), arXiv:1606.04489 [astro-ph.HE].
- [20] G. Pagliaroli and F. L. Villante, *JCAP* **1808**, 035 (2018), arXiv:1710.01040 [hep-ph].
- [21] A. M. Taylor, S. Gabici, and F. Aharonian, *Phys. Rev. D* **89**, 103003 (2014), arXiv:1403.3206 [astro-ph.HE].
- [22] A. Palladino, X. Rodrigues, S. Gao, and W. Winter, (2018), arXiv:1806.04769 [astro-ph.HE].
- [23] N. Senno, K. Murase, and P. Meszaros, *Phys. Rev. D* **93**, 083003 (2016), arXiv:1512.08513 [astro-ph.HE].
- [24] M. G. Aartsen et al. (IceCube), *Science* **361**, 147 (2018), arXiv:1807.08794 [astro-ph.HE].
- [25] L. J. Kewley, M. A. Dopita, R. S. Sutherland, C. A. Heisler, and J. Trevena, *Astrophys. J.* **556**, 121 (2001), arXiv:astro-ph/0106324 [astro-ph].
- [26] C. Rojas-Bravo and M. Araya, *Mon. Not. Roy. Astron. Soc.* **463**, 1068 (2016), arXiv:1608.04413 [astro-ph.HE].
- [27] M. Ackermann et al. (Fermi-LAT), *Astrophys. J.* **755**, 164 (2012), arXiv:1206.1346 [astro-ph.HE].
- [28] M. G. Aartsen et al. (IceCube), *Astrophys. J.* **833**, 3 (2016), arXiv:1607.08006 [astro-ph.HE].
- [29] M. G. Aartsen et al. (IceCube), (2017), arXiv:1710.01191 [astro-ph.HE].
- [30] M. G. Aartsen et al. (IceCube), *Phys. Rev. Lett.* **111**, 021103 (2013), arXiv:1304.5356 [astro-ph.HE].
- [31] C. Kopper (IceCube), *PoS ICRC2017*, 981 (2018), arXiv:1710.01191 [astro-ph.HE].
- [32] H. M. Niederhausen and Y. Xu (IceCube), *PoS ICRC2017*, 968 (2018), arXiv:1710.01191 [astro-ph.HE].
- [33] H. Yuksel, M. D. Kistler, J. F. Beacom, and A. M. Hopkins, *Astrophys. J.* **683**, L5 (2008).
- [34] H. Abdalla et al. (H.E.S.S.), Submitted to: *Astron. Astrophys.* (2018), arXiv:1806.03866 [astro-ph.HE].
- [35] R. C. Gilmore, R. S. Somerville, J. R. Primack, and A. Dominguez, *Mon. Not. Roy. Astron. Soc.* **422**, 3189 (2012), arXiv:1104.0671 [astro-ph.CO].
- [36] V. Berezhinsky and O. Kalashev, *Phys. Rev. D* **94**, 023007 (2016).
- [37] M. Ackermann et al. (Fermi-LAT), *Phys. Rev. Lett.* **116**, 151105 (2016), arXiv:1511.00693 [astro-ph.CO].
- [38] M. Lisanti, S. Mishra-Sharma, L. Necib, and B. R. Safdi, *Astrophys. J.* **832**, 117 (2016), arXiv:1606.04101 [astro-ph.HE].
- [39] H.-S. Zechlin, A. Cuoco, F. Donato, N. Fornengo, and M. Regis, *Astrophys. J.* **826**, L31 (2016), arXiv:1605.04256 [astro-ph.HE].
- [40] M. Di Mauro, F. Calore, F. Donato, M. Ajello, and L. Latronico, *Astrophys. J.* **780**, 161 (2014), arXiv:1304.0908 [astro-ph.HE].
- [41] M. G. Aartsen et al. (IceCube), *Astrophys. J.* **835**, 151 (2017), arXiv:1609.04981 [astro-ph.HE].
- [42] G. E. Romero, A. L. Müller, and M. Roth, *Astron. Astrophys.* **616**, A57 (2018), arXiv:1801.06483 [astro-ph.HE].
- [43] A. Aab et al. (Pierre Auger), *Astrophys. J.* **853**, L29 (2018), arXiv:1801.06160 [astro-ph.HE].
- [44] R. U. Abbasi et al. (Telescope Array), Submitted to: *Astrophys. J. Lett.* (2018), arXiv:1809.01573 [astro-ph.HE].
- [45] A. Palladino, M. Spurio, and F. Vissani, *JCAP* **1612**, 045 (2016), arXiv:1610.07015 [astro-ph.HE].
- [46] A. Albert et al. (IceCube, ANTARES), (2018), arXiv:1808.03531 [astro-ph.HE].
- [47] C. Haack and C. Wiebusch (IceCube), *PoS ICRC2017*, 1005 (2018), arXiv:1710.01191 [astro-ph.HE].

- [48] M. Ackermann et al. (Fermi-LAT), *Astrophys. J.* **799**, 86 (2015), arXiv:1410.3696 [astro-ph.HE].
- [49] R. Gandhi, C. Quigg, M. H. Reno, and I. Sarcevic, *Phys. Rev.* **D58**, 093009 (1998), arXiv:hep-ph/9807264 [hep-ph].
- [50] A. Palladino and W. Winter, *Astron. Astrophys.* **615**, A168 (2018), arXiv:1801.07277 [astro-ph.HE].
- [51] C. Gruppioni et al., *Mon. Not. Roy. Astron. Soc.* **432**, 23 (2013), arXiv:1302.5209 [astro-ph.CO].
- [52] D. Gaggero, A. Urbano, M. Valli, and P. Ullio, *Phys. Rev.* **D91**, 083012 (2015), arXiv:1411.7623 [astro-ph.HE].

## Supplementary material

The next sections are dedicated to more detailed calculations of *i)* the diffuse neutrino flux, *ii)* the expected number of events in the HESE and CAS<sub>4</sub> data sets and *iii)* the contribution from Normal Galaxies.

### Computation of diffuse neutrino flux

For hadronic, *i.e.* proton-proton, interactions the  $\gamma$ -ray and the all-flavor neutrino spectrum obey the following energy budget relation:

$$\int_0^\infty \frac{d\phi_\gamma}{dE} E dE \approx \frac{2}{3} \int_0^\infty \frac{d\phi_\nu}{dE} E dE \quad (2)$$

where  $\frac{dN}{dE}$  is the differential flux at the source. The diffuse neutrino flux expected from HAGS, we start from the  $\gamma$ -ray luminosity spectrum from a single source. We assume that it is a power law with a spectral index equal to  $\alpha+2$ , an energy cutoff  $E_{\text{cut}}$  and we denote it as  $\frac{d\mathcal{L}_\gamma}{dE}(E, E_{\text{cut}}, \alpha)$ . For each value of  $\alpha$ , the related neutrino spectrum is normalized in order to reproduce  $L_\nu = 3/2 L_\gamma^{\text{NGC } 253}$  in the energy range between 0.1 GeV and 3 TeV, since we take the Starburst Galaxy NGC 253 as a benchmark object in our calculation. This object has been recently observed by both Fermi-LAT and HESS [34]. Under the previous assumptions the neutrino flux from a single source is given by:

$$\frac{d\phi_\nu}{dE}(E, E_{\text{cut}}, \alpha, z) = \int_0^z dz \frac{d\mathcal{L}_\nu[E(1+z), E_{\text{cut}}, \alpha]}{4\pi D_c(z)^2 (1+z)^2 E^2} \quad (3)$$

We denote the neutrino flux from a single source with  $\phi(E_\nu)$ . where  $z_{\text{max}} = 6$ ,  $D_c(z) = D_H \times d(z)$  is the comoving distance,  $D_H$  is the Hubble distance and  $d(z) = \int_0^z dz h(z)^{-1}$ . In the previous equation the terms  $h(z) = \sqrt{\Omega_\lambda + \Omega_m(1+z)^3}$  with  $\Omega_\lambda = 0.73$  and  $\Omega_m = 0.27$ .

In order to obtain the cumulative neutrino flux we parameterize the evolution of the sources in redshift as in [33]:

$$\frac{dN}{dV}(z) = \rho_0 \left[ (1+z)^{a\eta} + \left(\frac{1+z}{B}\right)^{b\eta} + \left(\frac{1+z}{C}\right)^{c\eta} \right]^{1/\eta}, \quad (4)$$

where  $a = 3.4$ ,  $b = -0.3$ ,  $c = -3.5$ ,  $B = 5000$ ,  $C = 9$ ,  $\eta = -10$ . The parameter  $\rho_0$  denotes the local density of sources at redshift ( $z = 0$ ). In our case  $\rho_0(\alpha)$  is obtained by fitting data and depends on the spectral index (values are given in Tab.II). The diffuse neutrino flux is indicated using  $\Phi(E_\nu)$  and it is obtained from:

$$\frac{d\Phi_\nu}{dE_\nu}(E, E_{\text{cut}}, \alpha) = \int_0^{z_{\text{max}}} \frac{d\phi_\nu}{dE}(E, E_{\text{cut}}, \alpha, z) \frac{dN}{dV}(z, \alpha) \frac{dV}{dz} dz \quad (5)$$

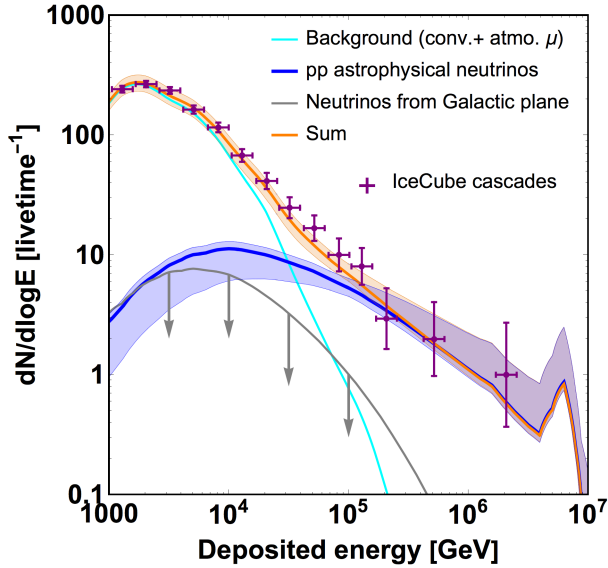


FIG. 4. Differential number of neutrino events in the Southern Sky compared to the 4-year cascade analysis (CAS<sub>4</sub>) [32]. The contribution from the pp model is shown for spectral indices  $1.9 \leq \alpha \leq 2.12$  by the blue band, assuming a flavor composition of  $\nu_e : \nu_\mu : \nu_\tau = 1 : 1 : 1$ . The atmospheric background (cyan) is taken directly from [32] and the galactic contribution (gray) from [19]. Due to the large statistical error above 200 TeV, the sensitivity to the shape of the astrophysical signal is low. This region is better constrained by the TGM sample.

where  $dV/dz$  gives the relation between the comoving volume and the redshift as follows,  $\frac{dV}{dz} = 4\pi D_H^3 \frac{d^2(z)}{h(z)}$ . We have chosen  $z_{\max} = 6$  in our calculations but we have checked that larger choices of  $z_{\max}$  do not produce any significant impact on the calculations.

### Computation of neutrino event counts

This section describes the methods how we compare our model with the IceCube data. The number of events expected in six years of the HESE data [31] is

$$N_{\text{ev}} = 4\pi T \int_0^\infty dE_\nu \frac{1}{3} \frac{d\Phi_\nu}{dE_\nu} \times \sum_i A_{\text{eff}}^i(E), \quad (6)$$

where  $T=5.7$  years,  $\Phi_\nu$  is the total neutrino flux. We assume the equipartition of flavors  $i$  at Earth ( $\nu_e : \nu_\mu :$

$\nu_\tau = 1 : 1 : 1$ ) and  $A_{\text{eff}}^i(E)$  is the effective area for  $\nu_i$  [1].

For the CAS<sub>4</sub> sample, we compute the differential event distribution by using

$$\frac{dN_{\text{ev}}}{dE_{\text{dep}}} = 2\pi T \left[ \frac{dN_{\text{ev}}^{\text{CC}}}{dE_{\text{dep}}}(E_{\text{dep}}) + \frac{dN_{\text{ev}}^{\text{NC}}}{dE_{\text{dep}}}(E_{\text{dep}}) \right]. \quad (7)$$

The dominant first term represents the contribution from charged current interactions  $\nu_\ell + \text{nucleons} \rightarrow \ell + X$ , which is

$$\frac{dN_{\text{ev}}^{\text{CC}}}{dE}(E) = \eta A_{\text{eff}}^e(E) \phi_\nu^\ell(E) + \eta A_{\text{eff}}^\tau \left( \frac{E}{\xi_\tau} \right) \phi_\nu^\ell \left( \frac{E}{\xi_\tau} \right).$$

The second term

$$\frac{dN_{\text{ev}}^{\text{NC}}}{dE}(E) = (1 - \eta) \sum_{\ell=e,\mu,\tau} A_{\text{eff}}^\ell \left( \frac{E}{\xi_{\text{NC}}} \right) \phi_\nu^\ell \left( \frac{E}{\xi_{\text{NC}}} \right)$$

describes the contribution from neutral current interactions. The parameter  $\eta \simeq 0.75$  is the ratio between the charged current cross section and the total deep inelastic scattering cross section. It is approximately constant in the energy region of interest [49]. The parameters  $\xi_\tau = 0.7$  and  $\xi_{\text{NC}} = 0.25$  give the relation between deposited energy and incident energy for CC interactions of  $\nu_\tau$  and all neutrino flavors interacting via NCs, respectively [50]. The best fit (orange curve) is compared to the data in Figure 4. The orange band comes from the different spectral indices that have been used, i.e.  $1.9 \leq \alpha \leq 2.12$ .

### Gamma-rays and neutrinos from Normal Galaxies

Normal galaxies, such as ours, are more abundant but less luminous than HAGS. Therefore it might be important to estimate their contribution to the diffuse  $\gamma$ -ray and neutrino fluxes, using the same procedure as for HAGS. As a typical luminosity of normal galaxy we use that of the Milky Way  $\sim 10^{39}$  erg/s in the 0.1 GeV - 3 TeV energy range [26]. The local density is estimated as  $\rho_0 = 10^{-2.7}$  Mpc<sup>-3</sup> from *HERSCHEL* data (Figure 4 of [51]). The spectral index is varied in the range  $\alpha \in [2.4 - 2.7]$ , which includes the rather extreme KRA- $\gamma$  model [52] and that of galactic cosmic-rays. The resulting diffuse fluxes from normal galaxies are presented in Figure 5 for the range of spectral indices. Even for the hardest spectral indices the contribution to the EGB and the neutrino flux is at level of few %.

TABLE II. Summary of our main results. In the table the values of different parameters are reported, namely: the energy cutoff  $E_{\text{cut}}^*$  in units of PeV, the local source density  $\rho_0(\alpha)$  in units of  $\text{Mpc}^{-3}$ , the contribution to the extragalactic  $\gamma$ -ray background as a function of the spectral index  $\alpha$ . The parameter  $\rho_0(\alpha)$  denotes the local density of sources that is required to power the TGM energy flux. Here we show two different examples, assuming as a prototype source NGC 253 and ARP 220. In the last three columns on the right we write what is the tension between the contribution to the EGB expected from our model and the results of the three calculations discussed in the paper [37–39].

$\alpha$	$E_{\text{cut}}^*$	NGC 253		ARP 220		Contribution to			Tension with		
		$\rho_0(\alpha)$	$\rho_0(\alpha)$	$\rho_0(\alpha)$	$\rho_0(\alpha)$	total EGB	Fermi coll. [37]	Lisanti et al. [38]	Zechlin et al. [39]		
1.9	3.2	$7.7 \times 10^{-5}$	$5.1 \times 10^{-7}$			6%	no	no	no		
2.0	4.1	$2.3 \times 10^{-4}$	$1.6 \times 10^{-6}$			11%	no	no	no		
2.1	5.1	$7.9 \times 10^{-4}$	$5.3 \times 10^{-6}$			25%	$0.8\sigma$	no	$0.3\sigma$		
2.12	5.3	$1.0 \times 10^{-3}$	$6.7 \times 10^{-6}$			28%	$1\sigma$	no	$0.5\sigma$		
2.2	6.3	$2.8 \times 10^{-3}$	$1.8 \times 10^{-5}$			50%	$2.6\sigma$	$2.1\sigma$	$1.7\sigma$		
2.3	7.8	$1.1 \times 10^{-2}$	$7.2 \times 10^{-5}$			100%	$6.9\sigma$	$8.7\sigma$	$4.8\sigma$		

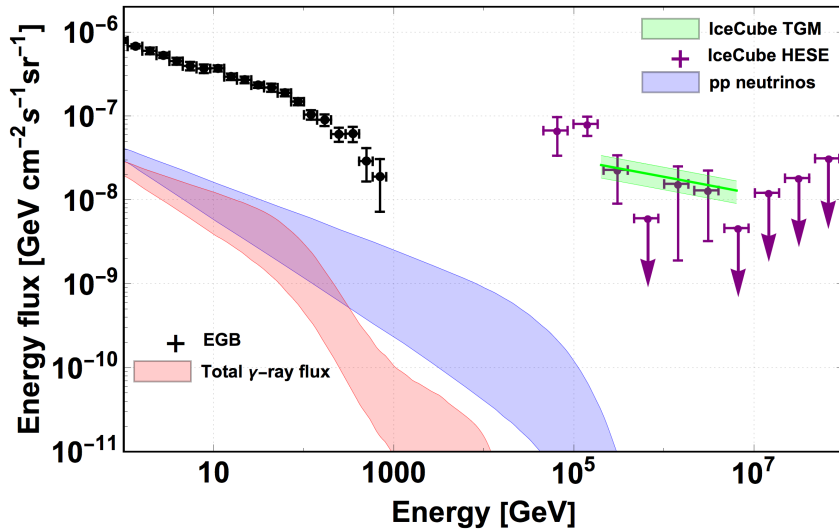


FIG. 5.  $\gamma$ -rays (red band) and neutrinos (blue band) produced by normal galaxies. The contribution to the EGB and to the IceCube flux is few %, therefore normal Galaxies cannot be the dominant class of HAGS.